Experimental Evidence of Thermal Vibrational Convection in a Nonuniformly Heated Fluid in a Reduced Gravity Environment

A. Mialdun, I. I. Ryzhkov, D. E. Melnikov, and V. Shevtsova

Microgravity Research Center, Université Libre de Bruxelles, CP–165/62, Avenue F.D. Roosevelt, 50, B–1050 Brussels, Belgium

(Received 17 December 2007; published 19 August 2008)

We report experimental evidence of convection caused by translational vibration of nonuniformly heated fluid in low gravity. The theory of vibrational convection in weightlessness is well developed but direct experimental proof has been missing. An innovative point of the experiment is the observation of a temperature field in the front and side views of the cubic cell. In addition, particle tracing is employed. The evolution of this field is studied systematically in a wide range of frequencies and amplitudes. The flow structures reported in previous numerical studies are confirmed. The transition from four-vortex flow to the pattern with three vortices is observed in the transient state.

DOI: 10.1103/PhysRevLett.101.084501 PACS numbers: 47.20.Ky, 42.40.Kw, 44.27.+g, 46.40.−f

Vibrational convection refers to the specific flows that appear when a fluid with a density gradient is subjected to external vibration. The density gradient may result from the inhomogeneity of temperature or composition. The case of small amplitude and high-frequency vibration (when the period is much smaller than the reference hydrodynamic times) is of special interest. In this case, the flow field can be decomposed into the "quick" part, which oscillates with the frequency of vibration, and the "slow" time-average part (mean flow), which describes the nonlinear response of the fluid to a periodic excitation [1]. This effect is most pronounced in the absence of other external forces (in particular, static gravity).

The study of vibrational impact on fluids has fundamental and applied importance. Vibrational convection provides a mechanism of heat and mass transfer due to the existence of mean flows. In weightlessness, it is an additional way of transporting heat and matter similar to thermo- and solutocapillary convection. Mean flows show some similarity with gravity-induced convection and might serve as a way to control and operate fluids in space [2]. Vibrations can suppress or intensify gravitational convection depending on the mutual orientation of vibration axis and thermal (compositional) gradient [3,4].

When a fluid is subjected to high-frequency vibration and density inhomogeneity is caused by the thermal gradient, the vibrational and gravitational convective mechanisms are characterized by the dimensionless parameters

$$\mathrm{Gs} = \frac{(A\Omega\beta_T\Delta T L)^2}{2\nu\chi}, \qquad \mathrm{Ra} = \frac{g\beta_T\Delta T L^3}{\nu\chi}, \quad (1)$$

where A is the amplitude of vibration, $\Omega = 2\pi f$ is the angular frequency, g is the gravitational acceleration, β_T is the thermal expansion, ν is the kinematic viscosity, χ is the thermal diffusivity, L is the characteristic size, and ΔT is the applied temperature difference. In (1), Ra is the Rayleigh number and Gs is known as its vibrational analogue. We suggest calling it the Gershuni number to mark a significant contribution of G. Z. Gershuni to the theory of thermovibrational convection [1]. The ratio Gs/Ra describes the relative importance of thermovibrational and gravitational convective mechanisms.

There have been extensive *theoretical* studies of thermovibrational convection in weightlessness and ground conditions. The fundamental treatise [1] comprises a systematic study of convective flows induced by high and finite frequency vibrations in closed and infinite cavities. Thermovibrational convection in square, rectangular, and cubic cavities was widely investigated providing a variety of mean flow structures and bifurcation scenarios [5–8]. Influence of vibration on double diffusive convection with the Soret effect was analyzed in [9].

The *experimental* studies of vibrational impact on the fluids in ground conditions were performed in a number of works. The considered configurations include vertical and horizontal layers [10], cavities subjected to nontranslational vibrations [11], Hele-Shaw cell [12], etc. At the same time, experiments addressing thermovibrational phenomena in low gravity are very limited. The only known series of experiments was carried out with the ALICE-2 instrument onboard MIR station [13,14]. The influence of vibration on the propagation of a temperature wave from a heat source in a near-critical fluid was investigated. The thermovibrational flows were registered by observing the optical inhomogeneity caused by the distortion of the temperature field. It was not possible to reconstruct this field quantitatively.

In this Letter, we report an experimental study of thermovibrational convection in low gravity. The fluid is placed in a cubic cell with differentially heated walls and subjected to translational vibration perpendicular to the temperature gradient (Fig. 1). This configuration was studied theoretically in weightlessness as well as ground conditions in a large number of works; see [1,5,6,8] and references therein. However, to the best of our knowledge, no experiments have been performed to evaluate these

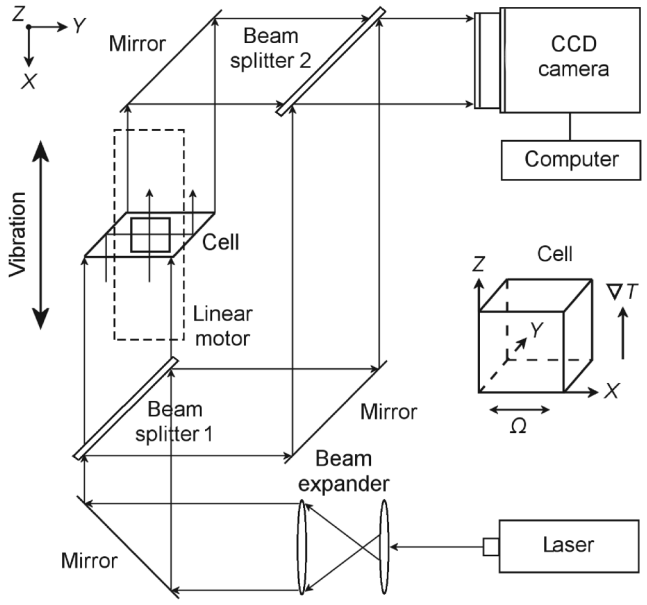

FIG. 1. The experimental setup.

results. The aim of the present experiment is to observe thermovibrational flows in low gravity and verify the existing theoretical studies. The experiments were performed in parabolic flights during the 46th campaign organized by the European Space Agency. Parabolic flights provide repeated periods of approximately 20 seconds of reduced gravity $g \sim 0.01 g_0$ preceded and followed by 20 seconds of hypergravity (up to $1.8 g_0$), where $g_0 = -9.81\ m/s^2$.

The design of the experimental setup is shown in Fig. 1. A cubic cell with transparent walls of size $L = 5$ mm is filled with isopropanol. A constant temperature difference ΔT is maintained between the opposite walls by the Peltier elements. The direction of the temperature gradient is perpendicular to the plane of Fig. 1 (see separate sketch of the cell). The mean temperature of the experiment was 40 °C. The physical properties of isopropanol at this temperature are $\beta_T = 1.095 \times 10^{-3}\ K^{-1}$, $\nu = 1.730 \times 10^{-6}\ m^2/s$, $\chi = 0.623 \times 10^{-7}\ m^2/s$. The thermal conductivities of the liquid and lateral walls are 0.13 and 1.3 W/mK, respectively. The cell is fixed to the linear motor, which performs translational harmonic oscillations in the X direction. The thermovibrational flows were monitored by measuring the temperature field inside the cell and recording the velocity field with help of isodense tracer particles (hollow ceramic microspheres with a diameter of 150 μm).

The temperature field is measured by optical digital interferometry [15]. The setup is based on the concept of the Mach-Zehnder interferometer; see Fig. 1. The light beam of a He-Ne laser ($\lambda = 633$ nm) is enlarged by the beam expander and split into two collimated beams of equal intensity by the beam splitter. One of them transverses the entire cell in two perpendicular directions. Two prisms at the side walls allow scanning the front and side views (planes YZ and XZ, respectively). The beam paths through the cell are shown by arrows. The temperature variations in the liquid create the spatial distribution of refractive index that modulates the wave front of the emerging optical beam. After passing the mirror, this beam interferes with the reference one at the second beam splitter. The resulting pattern is recorded by CCD camera (24 fps). The fringe images are processed by performing 2D fast Fourier transform, filtering the selected band of the spectrum, performing the inverse transform, and phase unwrapping. The knowledge of the phase shift gives information about the gradient of refractive index, which is used to reconstruct 2D projections of the temperature field on the front and side view planes. The temperature is measured with an accuracy of 0.01 K. Note that two views allow one to determine the exact positions of particles in the cell. The experimental setup was installed in the aircraft in such a way that the X and Y axes were in the plane of the wings (positive X axis pointed towards the nose). The Z axis was perpendicular to the wings going out the upper side of the vehicle. The microgravity level during parabolas is $|g_{X,Y}/g_0| \leq 0.01$, $|g_Z/g_0| \leq 0.05$.

The scenario of the experiment is as follows. The temperature gradient is established in the cell during horizontal flight. To minimize gravitational convection, the cell is heated from above (the temperature gradient is opposed to the gravity vector). The vibration starts in the beginning of the microgravity period and continues for 25 s. During this time, the interferometric patterns are recorded by the camera. The viscous and thermal times of the system are $L^2/\nu = 14.5$ s and $L^2/\chi = 401.3$ s, respectively. It makes it possible to observe the transient development of thermovibrational flow and its influence on the temperature field during 20 s of microgravity. In the experiments, the frequency and amplitude were varied in the ranges 1–12 Hz and 10–140 mm, respectively. The maximum vibrational acceleration of $5.8 g_0$ was achieved at $A = 10$ mm and $f = 12$ Hz. The upper limit for frequency increases with decreasing the amplitude.

The first picture from the left in Fig. 2(a) shows the temperature field in the cell (side view) at the end of the parabola when no vibration is applied. There are some deviations from a conductive state, which are small in the central region of the cell but become larger near the lateral walls due to heat fluxes through them. Note that the walls are formed by two glass prisms, which can absorb heat. Another reason for temperature deviations is the weak convection caused by the residual gravity. The residual accelerations in the X and Y directions (perpendicular to the thermal gradient) can slightly destabilize vibrational mean flows, while their influence in the Z direction can be stabilizing or destabilizing depending on the sign of g_Z. The analysis of different parabolas showed that the deviations from a conductive state are not large. Note that thin regions (~0.2 mm) near the horizontal walls were inaccessible for optical measurements.

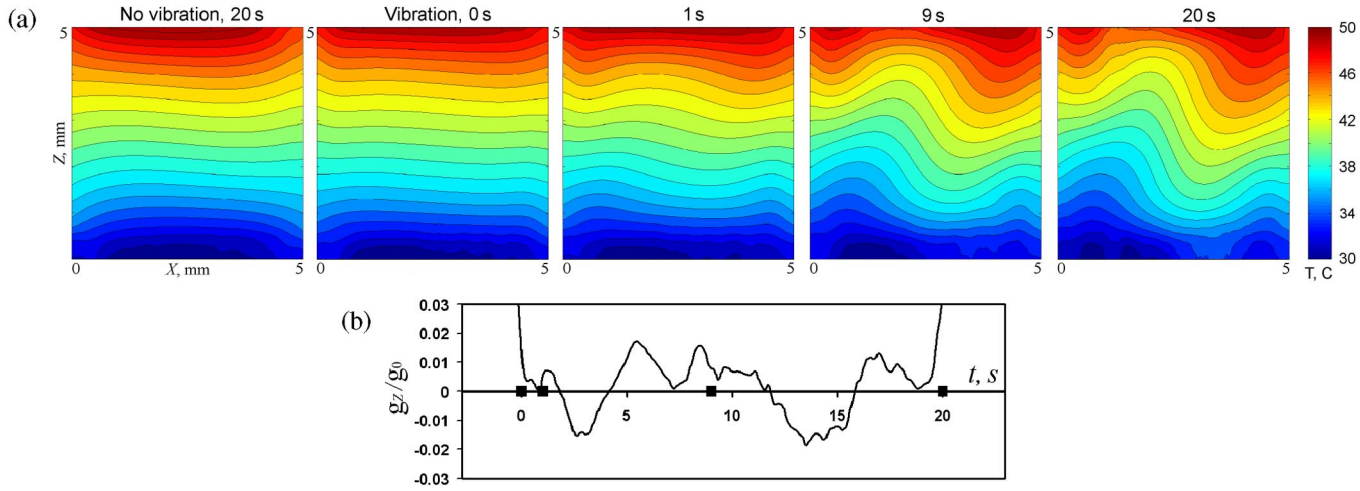

FIG. 2 (color online). (a) Temperature field in the side view when no vibration is applied (first picture) and its evolution during a parabola with vibration $f = 4$ Hz, $A = 45$ mm, $\Delta T = 20$ K, Gs = 71 149. (b) g_Z/g_0 gravity profile with four points indicating the times when the snapshots were taken.

The situation is strikingly different when vibration is applied to the system. In Fig. 2(a), the evolution of the temperature field in the side view is shown during the parabola with vibrational impact of $f = 4$ Hz, $A = 45$ mm, and temperature difference $\Delta T = 20$ K. These images are recorded at different times but correspond to the same phase of vibration, in which the cell was in the focus of the camera. It should be noted that our preliminary numerical simulations as well as the previous results [16] showed that the oscillatory distortion (quick part) of the temperature field is very small with respect to the time-averaged distortion induced by the mean flow. So, the patterns in Fig. 2(a) represent the mean temperature field with a good accuracy. In the presented configuration, the Gershuni number is Gs = 71 149, while $\mathrm{Gs}/\mathrm{Ra}_{X,Y} = 28.6$ and $\mathrm{Gs}/\mathrm{Ra}_Z = 14.3$, where the Rayleigh numbers [see Eq. (1)] correspond to the maximum residual gravity along the axes: $|g_{X,Y}/g_0| < 0.01$, $|g_Z/g_0| < 0.02$. So, the vibrational convective mechanism is dominant and responsible for the observed change of temperature field. In the beginning of the parabola (0 s), the situation is close to the conductive state. The development of thermovibrational flow causes the distortion of the temperature field, which is growing with time. The bifurcation from a symmetric pattern (1 s) to an asymmetric one (9 and 20 s) is observed. This result verifies the previous numerical simulations [1,5,8]. In these studies, it was found that for Gershuni numbers below the critical value (for the present configuration, $\mathrm{Gs}_{cr} = 15\mathrm{x}10^3$), a four-vortex pattern [Fig. 3(a)] is established at the steady state. Above the critical value, this pattern becomes metastable; the time of its existence decreases with increasing the Gershuni number. With time, the transition to the steady state with one big vortex and two small vortices occurs [Fig. 3(b)]. We have observed this transition experimentally. The snapshots on Fig. 2 clearly demonstrate the four-vortex pattern at $t = 1$ s. It exists during the first two seconds and is replaced by one big diagonal vortex at $t = 3$ s (one-fifth of the viscous time). The images taken at 9 and 20 s clearly show this structure.

In Fig. 4, two perpendicular views of the cell are presented at the end of the microgravity time. This figure underlines the advantage of two simultaneous views. The flow is developing in the XZ plane formed by the directions of vibration and temperature gradient (side view). The

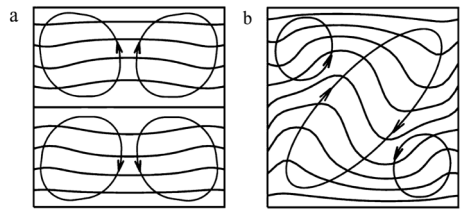

FIG. 3. Flow structures and isotherms obtained by numerical simulations. (a) $\mathrm{Gs} = 7 \times 10^3$ [8], (b) $\mathrm{Gs} = 70 \times 10^3$ [1,5].

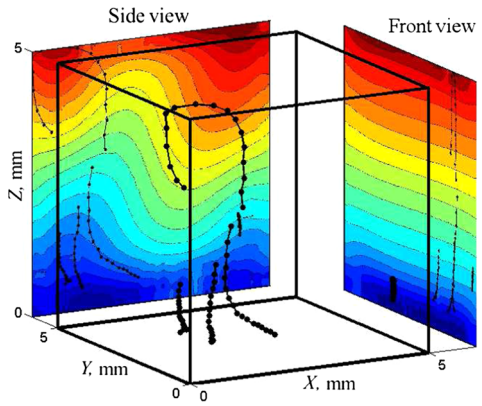

FIG. 4 (color online). Temperature field (side and front views) at the end of a parabola. The trajectories of particles and their projections on the planes XZ and YZ are also shown.

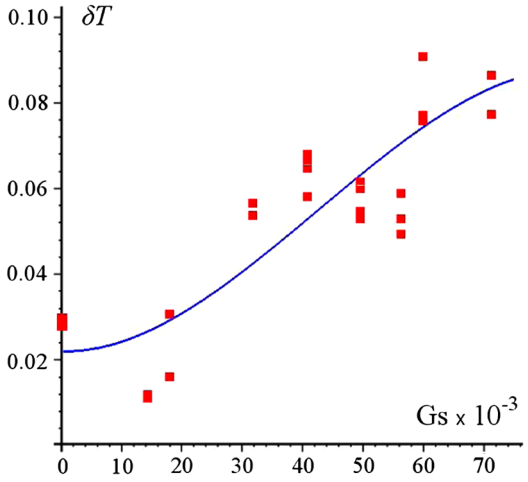

FIG. 5 (color online). Temperature deviation vs Gs (i.e., the intensity of mean flow as a function of periodic excitation).

distortion of the temperature field in the front view is small. Note that this field is a superposition of patterns in the planes of constant X. Because of the specific structure of the side view pattern, an interchange of higher and lower temperature regions occurs when one moves in the X direction at fixed Y and Z. It explains the obtained front view pattern. We found that the distance between the isotherms in the central part of the cell was slightly increasing with time, while near the top and bottom walls the isotherms were approaching each other. It is supported by the results of numerical simulation [8]. The trajectories of several particles are also presented in Fig. 4. They confirm the expected structure of mean flow shown in Fig. 3(b). The velocity in the vertical direction measured by digital particle tracing velocimetry is about 0.5 mm/s. It agrees well with numerical results [8] that predict a maximal vertical velocity of 0.3 mm/s for the present configuration (without residual gravity).

The collective results of numerous experiments are demonstrated in Fig. 5. To characterize the intensity of mean flow, the average temperature deviation from the conductive profile (observed in the absence of vibration) is introduced:

$$\delta T = \frac{1}{\Delta T L} \int_0^L |T - T_{\mathrm{cond}}|_{x=L/2} dZ.$$

This deviation is calculated at the end of the parabola and plotted as a function of Gershuni number. The solid curve outlines the tendency in this dependence. We have found that for Gershuni numbers below the critical value of $\mathrm{Gs}_{\mathrm{cr}} = 15 \times 10^3$, the thermal pattern is close to that of Fig. 3(a), which agrees with the numerical results [1]. The flow is weak and does not change much with Gs number while $\mathrm{Gs} < \mathrm{Gs}_{\mathrm{cr}}$. The influence of residual gravity is rather large here. As the Gershuni number increases, the thermal deviation grows indicating the dominant role of vibration. The scattering of the experimental points is attributed to the quality of the parabolas.

Finally, several experiments were carried out in normal gravity for various vibrational excitations. The gravity drastically suppresses vibrational convection; the distortion of isotherms was even smaller than in the case $f = 0$ (see Fig. 2). For comparison, $\delta T \sim 0.008$ for $\mathrm{Gs} = 50 \times 10^3$ in normal gravity.

To summarize, we have reported the first direct experimental evidence of thermovibrational convection in low gravity. The temperature field in the fluid is measured in two perpendicular directions, and its evolution is investigated systematically in a wide range of frequencies and amplitudes. The transition between two structures of mean flow predicted by theory is demonstrated. A strong heat transport attributed to the mean flow is found under vibration in low gravity. This transport is significantly weaker in the absence of vibration (only residual gravity) and negligibly small in normal gravity for the studied levels of vibration.

This work is supported by the PRODEX program of the Belgian Federal Science Policy Office.

[1] G. Z. Gershuni and D. V. Lyubimov, *Thermal Vibrational Convection* (Wiley & Sons, New York, 1998).
[2] D. Beysens, Europhysics News **37**, 22 (2006).
[3] R. Savino and R. Monti, in *Physics of Fluids in Microgravity* (Taylor & Francis, London, 2001), p. 178.
[4] V. A. Demin, G. Z. Gershuni, and I. V. Verkholantsev, Int. J. Heat Mass Transf. **39**, 1979 (1996).
[5] G. Z. Gershuni, E. M. Zhukhovitskii, and Y. S. Yurkov, Fluid Dyn. **17**, 565 (1982).
[6] K. Hirata, T. Sasaki, and H. Tanigawa, J. Fluid Mech. **445**, 327 (2001).
[7] I. Cisse, G. Bardan, and A. Mojtabi, Int. J. Heat Mass Transf. **47**, 4101 (2004).
[8] R. Savino, R. Monti, and M. Piccirillo, Comput. Fluids **27**, 923 (1998).
[9] V. Shevtsova, D. Melnikov, J. C. Legros, Y. Yan, Z. Saghir, T. Lyubimova, G. Sedelnikov, and B. Roux, Phys. Fluids **19**, 017111 (2007).
[10] M. P. Zavarykin, S. V. Zorin, and G. F. Putin, Dokl. Akad. Nauk SSSR **299**, 309 (1988).
[11] A. A. Ivanova and V. G. Kozlov, Fluid Dyn. **38**, 372 (2003).
[12] I. A. Babushkin and V. A. Demin, J. Appl. Mech. Tech. Phys. **47**, 183 (2006).
[13] A. V. Zyuzgin, A. I. Ivanov, V. I. Polezhaev, G. F. Putin, and E. B. Soboleva, Cosmic Res. (Transl. of Kosm. Issled.) **39**, 175 (2001).
[14] Y. Garrabos, D. Beysens, C. Lecoutre, A. Dejoan, V. Polezhaev, and V. Emelianov, Phys. Rev. E **75**, 056317 (2007).
[15] A. Mialdun and V. Shevtsova, Int. J. Heat Mass Transf. **51**, 3164 (2008).
[16] R. Monti, R. Savino, and G. Alterio, Acta Astronomica **40**, 369 (1997).